Optical feedback implementation for polymer based tunable laser

Master's Thesis of

Tianwen Qian

at the Karlsruhe School of Optics & Photonics
in cooperation with Fraunhofer Heinrich-Hertz-Institut

July 2018 – December 2018

Karlsruhe Institute of Technology
Karlsruhe School of Optics & Photonics
Schlossplatz 19
76131 Karlsruhe | Germany

I herewith declare that the present thesis is original work written by me alone, that I have indicated completely and precisely all aids used as well as all citations, whether changed or unchanged, of other theses and publications, and that I have observed the KIT Statutes for Upholding Good Scientific Practice, as amended.

Karlsruhe, 30.12.2017

....

(Tianwen Qian)

Abstract

The optical feedback introduced improvement on laser linewith and bandwidth has drawn a significant interest for the researchers.

In practice external feedback when coupled into the laser cavity through the output facet, causes a modification of the photon density. This perturbation leads to a fluctuation in the carrier density affecting the optical gain. Since the fluctuations of optical refractive index are directly related to the carrier density [11], the external feedback also introduces phase fluctuations. The interaction of the intensity and phase fluctuations makes the dynamics of the laser system under self-injection very complex leading to system instabilities and even chaos. [Kechaou, Grillot et al 2012]

As high-speed fiber-optic communication becomes increasingly important, so does the need to perform precision measurements on lasers and lightwave systems.

Contents

1. Introduction

The focus of this thesis is the study of the optical feedback effects on polymer-based tunable laser in order to improve its performance in linewidth and bandwidth. The tunable laser is constructed by a hybrid approach combining polymer-based photonic integrated circuits (PIC) and active Indium Phosphide (InP) components.

Semiconductor laser diodes with wide direct modulation bandwidth represent a relevant element to fulfill the continuously increasing need for low-cost optical communications systems with high bit-rate.

For the design process a set of three masks is needed, corresponding to the electrode, waveguide and air trench geometry.

The goal of this work is to analyze and improve the characteristics of the laser under feedback condition. Parameters measured by different set-ups for the characterization are presented in chapter 3. The samples produced based on this work are then characterized using optical transmission and reflection measurements. The measurements of these lasers, consisting of testing the designs, the application of different tuning principals and tuning experiments, are presented.

2. Theory of Laser Coupled with Passive Cavity

Semiconductor lasers with external cavities exhibit a variety of dynamical phenomena, depending on key parameters, comprising feedback strength, feedback delay, pump current, feedback type, and laser nonlinearity[]. Among all of them the, feedback sensitivity of laser diodes is governed essentially by the feedback parameters C, X and κ_{ext}. In order to correct consider the feedback effect a three-mirror laser model is considered in Figure 2.1.
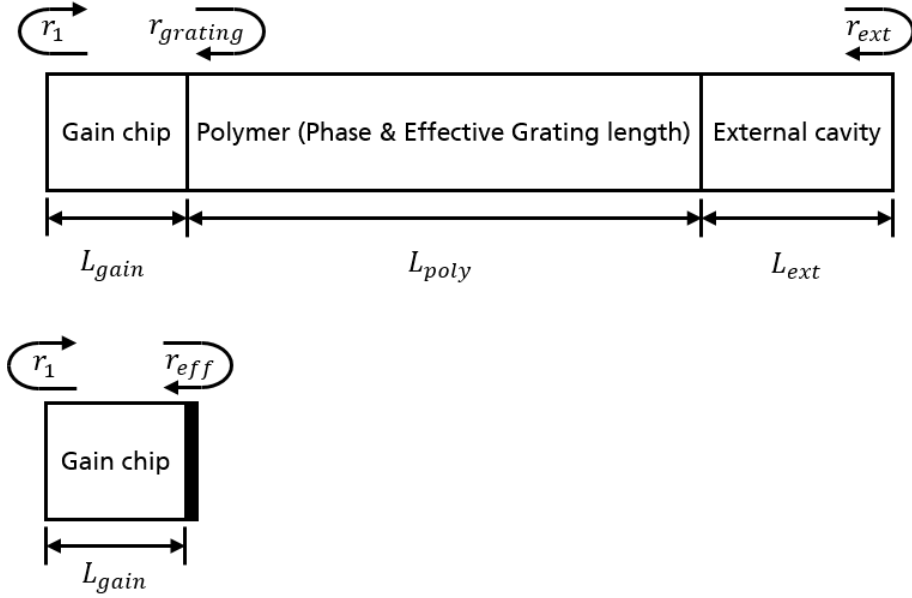
Figure 2.1.: External cavity laser and equivalent cavity with effective mirror to model the external section.

The feedback coefficient, C, characterizes the level of feedback in relation to how it affects the mode structure of the laser, is defined as

$$C = X\sqrt{1 + \alpha^2} \tag{2.1}$$

with

$$X = \frac{\tau_{ext}}{\tau_{gain} + \tau_{poly}}\kappa_{ext} \tag{2.2}$$

$$\kappa_{ext} = \frac{r_{ext}}{r_{grating}}\left(1 - \left|r_{grating}\right|^2\right) \tag{2.3}$$

κ_{ext} is the coupling coefficient from the grating reflector to the external cavity.

The C parameter indicates the laser stability under feedback is affected both by external reflector r_{ext} and external round-time delay τ_{ext}. When $C < 1$, usually for weak feedback and relatively short external cavityies, the laser operates in a single mode lasing region and is phase dependent to the external feedback, when $C > 1$, over one stable mode will appear and the laser will undergo a route-to-chaos behavior until it reaches coherence-collapse [] region, which is the region IV for the experimentally identified five distinct regimes of laser performance under feedback [1], if the feedback strength is even higher, the laser will become stable single mode again lasing with the compound cavity mode.

Rate equation models of the field and phase including the time delay of the feedback field reveal unstable solutions and chaotic behavior at these high feedback levels [1]. The collapse begins at the transition to regime IV, where the normally small satellite peaks created by noise-induced relaxation oscillations (depicted in Fig. 5.23) grow larger and larger, eventually becoming comparable to the central peak and broadening the linewidth dramatically [2].

In general, to understand the static lasing behavior under feedback is useful to consider the three-mirror cavity and by the feedback coefficient C, it also relates to the linewidth reduction under weak feedback condition, which will be explained in Section 2.1. However, in order to understand the dynamic lasing behavior we can generally consider the three-mirror cavity as an equivalent two-mirror cavity (shown in Figure 2.1), which replaces the passive section by an effective mirror with reflectivity r_{eff}. The vale of r_{eff} is defined as:

$$r_{eff} = \frac{r_{grating} + r_{ext}W}{1 + r_{grating}r_{ext}W} \tag{2.4}$$

$$W = e^{-2\alpha_{poly}L_{ext}}e^{-2i\beta_{poly}L_{ext}}. \tag{2.5}$$

The resonance equation G for the effective laser cavity model is given by

$$G = r_1 e^{-2i\beta_{gain}L_{gain}}r_{eff} = |G|e^{i\varphi}. \tag{2.6}$$

Cavity modes are obtianed from Equation 2.6 for integer values of $\phi/2\pi$; for the lasing mode m at threshold we have

$$\left|G(\lambda_m, g_{m,A})\right| = G_m = 1, \ \varphi_m = 2m\pi \tag{2.7}$$

these two conditions allow to numerically find the lasing mode wavelength λ_m and the required active section gain $g_{m,A}$.

If no reflection exists at the active-passive interface ($r_2 = 0$) and r_3 is positive and real, then $\phi_{eff} = -2\beta_p L_p$, and $L_{eff} = L_p$.

2.1. Linewidth and Chirp Reduction

Linewidth and chirp reduction due to the optical feedback is related to the same factor F, which is given as [3]

$$F = 1 + \frac{1}{\tau_{gain}}\frac{d\phi_{r_{eff}}}{d\omega} + \frac{\alpha}{\tau_{gain}}\frac{d\ln r_{eff}}{d\omega} = 1 + A + B \tag{2.8}$$

$$A = \frac{1}{\tau_{gain}} \frac{d\phi_{r_{eff}}}{d\omega} \tag{2.9}$$

$$B = \frac{\alpha}{\tau_{gain}} \frac{d \ln r_{eff}}{d\omega} \tag{2.10}$$

because Equation 2.9 is the freqeuncy-derivative of the r_R phase, it denotes the effecitve round-trip time in the external cavity dived by τ_{in} []. That is, parameter A represents the ratio of the photon numbers outside to inside the gain medium. It remains nearly constant once the laser cavity is formed. However, parameter B, representing the slope of the spectral reflectivity, is changed if the lasing mode is detuned. Thus, it represents the contribution of the detuned loading effect which will be explained in Subsection 2.2.1.

If $\Delta\omega_0$ is denoted as the adiabatic chirp in the absence of feedback, then the chirp with external cavity $\Delta\omega$ is obtained as [3]

$$\Delta\omega = \frac{\Delta\omega_0}{F} \tag{2.11}$$

if the spectral linewidth without external feedback is denoted by $\Delta\nu_0$, the spectral linewidth with the external cavity $\Delta\nu$ is simply obtianed as []

$$\Delta\nu = \frac{\Delta\nu_0}{F^2} \tag{2.12}$$

Consider the different feedback regions, the reduction factor at weak feedback ($C < 1$) becomes

$$F = 1 + C\cos(\phi_{ext} + \arctan\alpha) \tag{2.13}$$

for strong feedback, which is more interesting and stable for the practical use, the factor F becomes

$$F = 1 + f_{ext}\frac{\tau_{ext}}{\tau_{gain} + \tau_{poly}} \tag{2.14}$$

According to this we can calculate the linewidth reduction factor F^2 versus the external cavity length as shown in Figure 2.2, which will be used for the device design in Section 4.1.

Table 2.1.: Parameters used in linewidth reduction factor F^2 calculation.

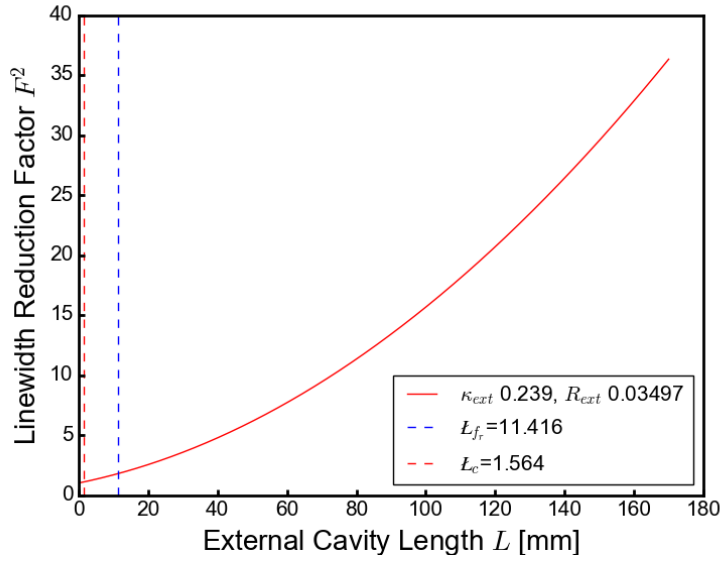| Symbol	Description	Value
L_{gain}	Active region length	300 μm
$L_{grating}$	Grating region length	699.84 μm
L_{poly}	Polymer region length	1224.84 μm
α	Linewidth redcution factor	-3
$R_{grating}$	Grating reflectivity	0.3
R_{ext}	External cavity reflectivity	0.187

Figure 2.2.: Linewidth reduction factor

2.2. Bandwidth Enhancement

The maximum bit-rate achieved by direct modulated lasers is typically limited by the well known resonance between carriers and photons [2], many solutions have been proposed to overcome this restriction. Three approaches to achieve broader bandwidth are explored in detail.

2.2.1. Detuned Loading Condition

The first mechanism identified to extend the modulation bandwidth of a semiconductor laser is the detuned loading effect that is due the dispersion effect introduced by a coupled cavity2,3 or by a distributed mirror (DBR4–6 or DFB7). It can be achieved when positioning the lasing mode at a slightly higher wavelength respect to the minimum threshold gain condition, which means the lasing mode of a DBR laser is oscillating at the slope of its grating response. It is reported that when the laser is operating at the longer wavelength side, the enhancement of modulation speed, reduction of phase noise (linewidth), and suppression of FM modulation (chirping) can be achieved [4]. The detuned loading of the laser cavity increases the interaction between the photons and the free carriers in the laser cavity [4] which will both increase the modulation bandwidth and reduce the variation of the carrier density during modulation [5]. This is because, in the longer wavelength region, the increase of the carrier density increases the material gain while reducing the mirror loss (i.e. increase the reflection from the grating). As a result, the effective differential gain is increased, which, in turn, reduces the effective linewidth enhancement factor [].
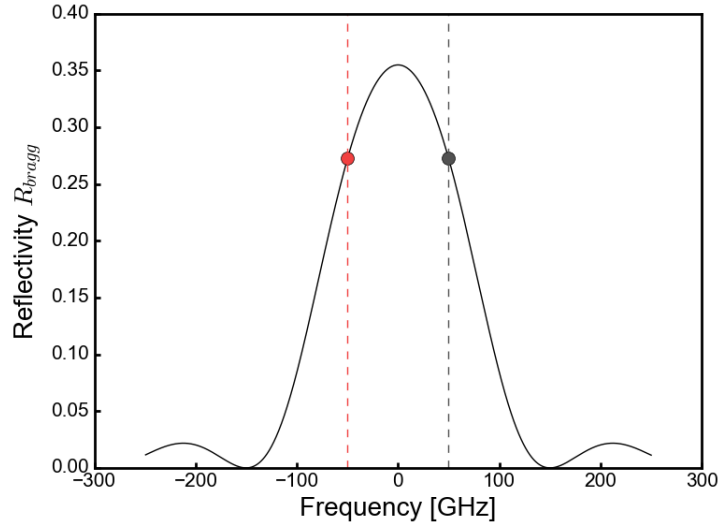
Figure 2.3.: Detuned loading condition with respect to the grating response. The red and grey dots correspond to the lasing mode detuend to the longer and shorter wavelength sides.

2.2.2. Undamped Relaxation Oscillation

Relaxation oscillation in a semiconductor laser occurs because the carrier cannot follow the photon decay rate, it usually smoothly decays out as long as the disturbance (e.g. external feedback) is small enough [6]. However, it can become undamped when the laser exhibits the feedback from the chip facet, which even influences the optical spectra that the undamping peaks are appearing beside the main mode with the mode spacing of relaxation frequency (typically 1~10 GHz). The undamped relaxation oscillation occurs for the appropriate combinations of feedback phase and strength as shown in Figure 2.4. The satellite peaks first appear as Figure 3.8 (b) and then slowly increase their intensity and move towards the main peak, follows with more satellite peaks appearing when the corresponding relaxation oscillation frequency is decreasing. The mode spacing between the main mode and side mode in Figure 3.8 (b) is 11 GHz and decreases to 9 GHz in Figure 3.8 (a).

Since the incoming feedback acts like a perturbation for the normal laser which introduces the amplitude modulation, the undamped RO can be also called as self-modulation or self-pulsation. The mechanism of self-pulsation is analysed and discussed in [7] as "dispersive Q-switching". In order to explain the self-pulsations one usually assumes some kind of a Q-switching process, where the term Q-switching denotes a switching of the quality-factor of the laser cavity. If, due to some reason to be discussed later, an increase of optical power yields a decrease of optical loss (or an increase of optical gain) within the laser, the round trip gain G may become larger than unity, yielding an exponential increase of optical power, corresponding to the rising edge of a developing pulse. On the other hand an increased power yields an increasing consumption of carriers so that finally the carrier density is too low to maintain a unity roundtrip gain and therefore the
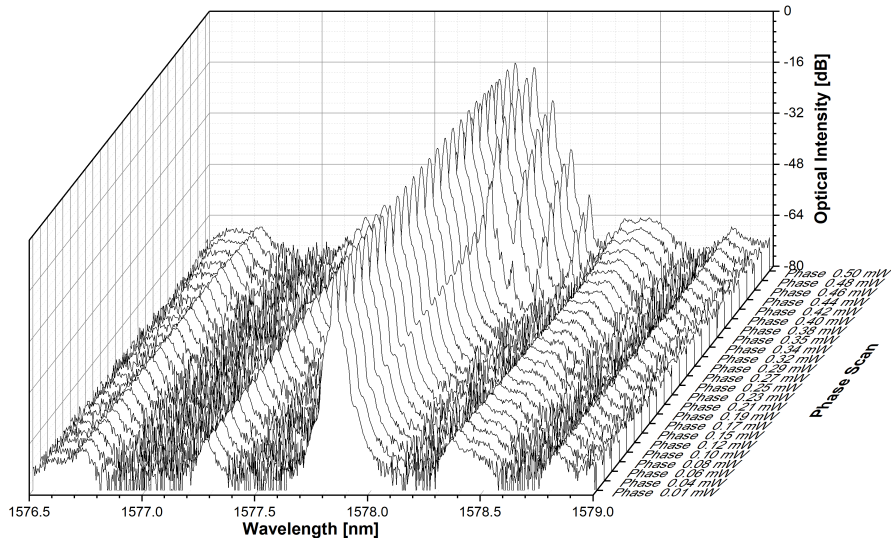
Figure 2.4.: Phase scan of the tunable laser spectra with feedback from chip facet. The side peaks of undamped RO start to appear with increasing of their intensity and shifting towards the main peak. While the applied phase current keep changing, more peaks due to undamped RO starts to appear until the laser shift to another mode and becomes stable single mode lasing again.

optical power collapses. A recovery time is required in order to increase the carrier density again until the next pulse develops. The repetition frequency for these pulses is of the same order as the relaxation resonance frequency [8].

2.2.3. Photon-Photon Resonance

Another approach used to extend the dynamic properties of an integrated laser is similar to detuned loading condition but in addition it takes advantage of the interaction between the lasing mode and an adjacent longitudinal cavity mode, properly separated in frequency in such a way they can interact due to the carrier pulsation introduced by the applied modulation signal at the gain section electrode. This interaction introduces a resonance in the impulse modulation (IM) response at the frequency corresponding to the modes separation. This resonance is frequently called Photon-Photon resonance (PPR), to distinguish this interaction mechanism respect to the Carrier-Photon resonance (CPR) [9]. The appearing of the PPR should not be too far away from the relaxation oscillation frequency so that the dip in between two peaks will not be deep enough to reach the -3 dB limation in the modulation response as shown in Figure 2.5.

The large enhancement of the modulation bandwidth, has been already observed to be closely related to a special behavior of the cavity round–trip phase (RTP) function [10]. Here we illustrate the operation principle using the same device parameter provided in [9], along with the python code for calculation, is shown in Section A.1.

The most favorable operation condition is when the lasing mode λ_0 operates in the detuned loaidng condition $\lambda_0 > \lambda_B$, the closest mode on other side respect to the Bragg wavelength λ_1 is strongly suppressed, and, finally, a mode on the same side respect to the
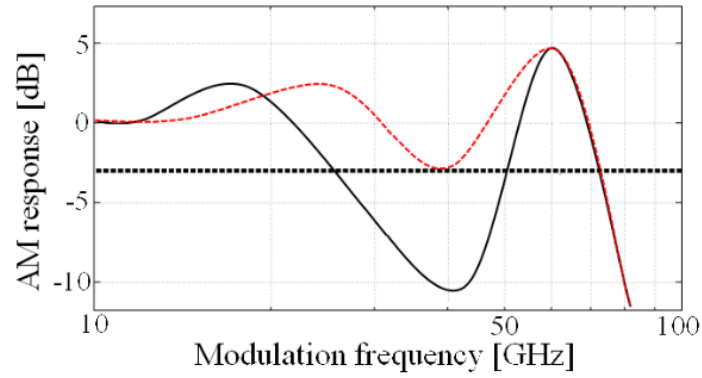
Figure 2.5.: Example of modulation responses obtained in cavity exploiting the PPR effect. The black line indicates a case in which the CP and the Photon–Photon peaks are too much separated whereas in the case indicated by the red line the modulation bandwidth extension is achieved [9].

Bragg wavelength λ_{-1} is placed on the the first lobe of the Round Trip Gain (RTG) curve. In this mode configuration, the PPR effect can arise due to the coupling between mode λ_0 and λ_{-1} [9]. In order to generate an adjacent longitudinal cavity mode under feedback, a strong feedback condition is required, which will form compound cavity modes with the mode spacing of the the normal cavity plus the external cavity.

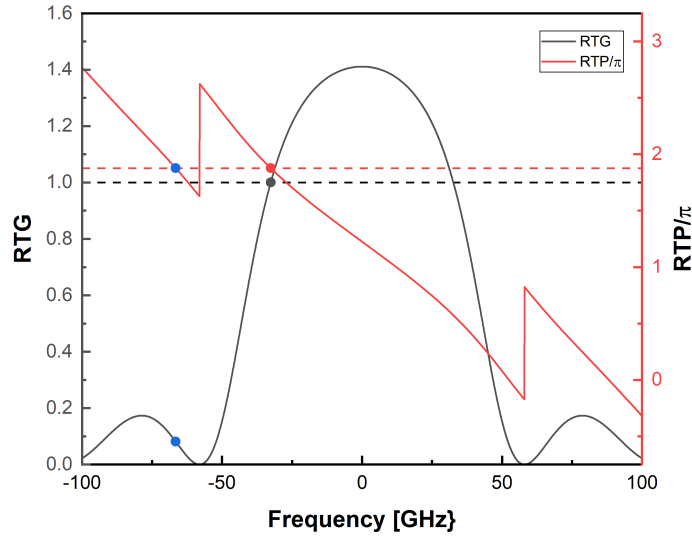$$\Delta v = \frac{c}{2(n_{gain}L_{gain} + n_{poly}L_{eff})} \tag{2.15}$$

Figure 2.6.: Round trip gain (RTG, grey curve) and phase (RTP, red curve) functions computed at the DBR threshold. The red marker represents the lasing mode Λ_0, the brown marker indicates the PPR mode λ_{-1}, the blue markers represent other non-lasing cavity modes, adapt from [9].

3. Tunable Laser with Reflection from Chip Facet

Characterization of the laser linewidth, RIN, bandwidth, α parameter and phase noise are measured with (1) Cleaved fiber with oil and (2) Lensed fiber, which corresponding to the laser without feedback and with feedback conditions. Principle of each measurement will be introduced and the results will be compared in the following sections.

All the measurements are done by fixing the gain section current $I_{gain} = 80\ mA$ and grating section current $I_{grating} = 15\ mA$, scanning the phase section from $0\ mA$ to $30\ mA$ with the step of $0.5\ mA$, each current step is considered as one index which leads to in total 61 index number. The scanning of the spectra and the examing of the side mode suppression ratio (SMSR) are shown in Figure 3.1. Due to the hysteresis effect the laser wavelength has a little shift under these two configurations, e.g. the mode hopping point in Figure 3.1 a) appears at index 51 and the correspoinding point in Figure 3.1 (b) is at index 48. Besides, the additional hopping behavior in Figure 3.1 (b) is due to the feedback effect since the undamped RO peaks appearing in the spectra. Important to note that the light grey points marked at the beginning of Figure 3.1 (c) are unstable working points with SMSR lower than 40 dB, several modes appeared at these phase currents and the laser performance dropped drastically, which can be seen from the α-factor measurement in Section 3.4.
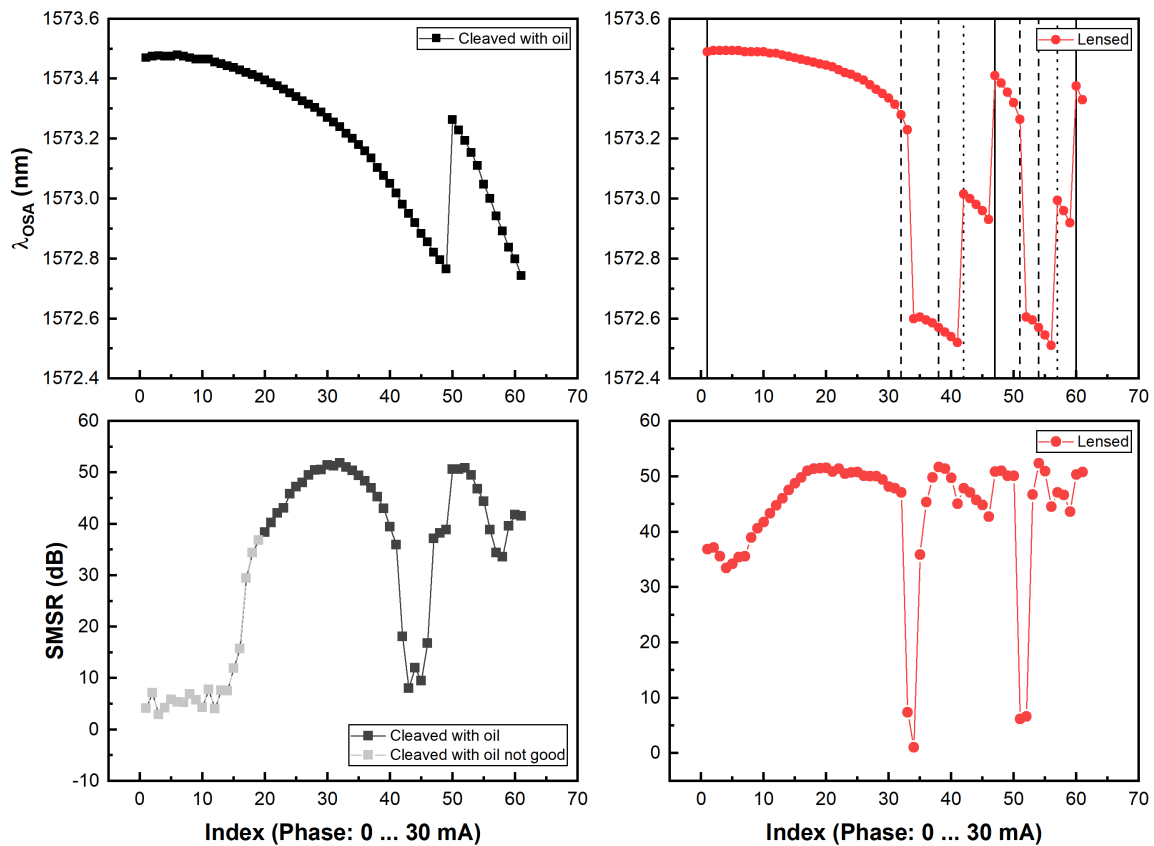
Figure 3.1.:

3.1. Linewidth Measurement

Laser linewidth is measured by self-homodyne method in the characterization. Self-homodyning can be described mathematically as a single-delay autocorrelation, which is shown in Figure 3.2, the optical spectrum at f_0 autocorrelates with the delayed version of itself to produce a time-fluctuating spectrum, whose detected voltage has a power spectrum centered at zero frequency. For the case of a laser with Lorentzian lineshape, the half-width of the detected spectrum is equal to the linewidth of the laser.

The self-homodyne measurement set-up is shown in Figure 3.3. The input directional coupler of the interferometer splits the light from the laser into two paths. One path is delayed in order to decorrelate the combinning signals, P_1 and P_2. The output coupler combines the two signals, which are then mixed at the photodectector of the lightwave signal analyzer. The homodyne power spectrum is then observed on the analyzer from which the Lorentzian linewidth is measured by placing a marker at the half power frequency.

The results of linewidth measurement are shown in Figure 3.4. Except for the unstable working points which are shown in light grey in Figure 3.4 (a), the laser linwidth under feedback become narrower than the case without feedback. It is due to the reason that the
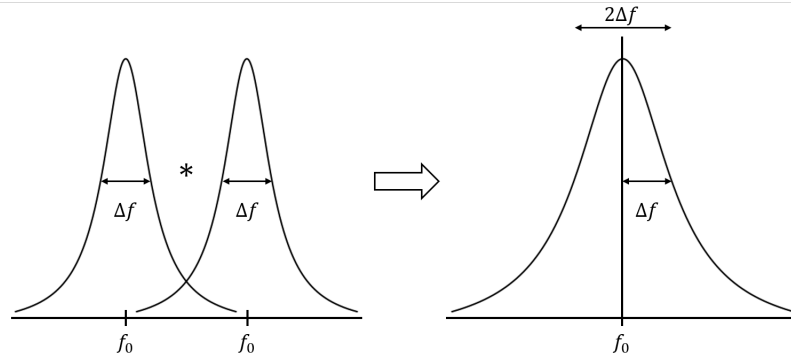
Figure 3.2.: Linewidth of a DBR laser using the self-homodyne technique. The optical spectrum at f_0 autocorrelates with the delayed version of itself to produce a time-fluctuating spectrum, whose detected voltage has a power spectrum centered at zero frequency, the half-width of the detected spectrum is equal to the linewidth of the laser.
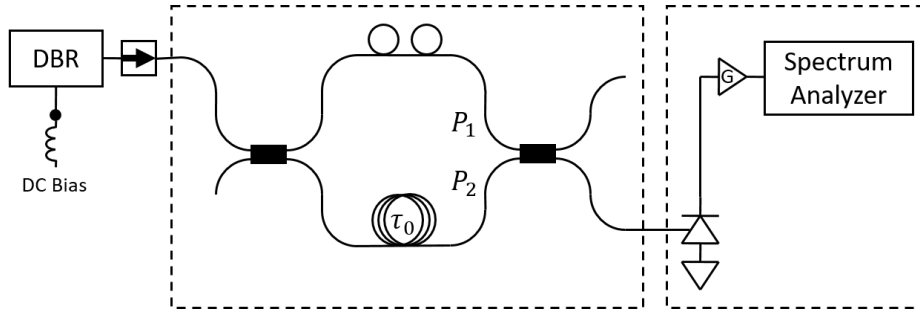

Figure 3.3.: Schematic set-up for self-homodyne linewidth measurement.

external refelctor formed by the polymer/air interface with $r_{ext} = 0.187$ is considered to be in the strong feedback region. In such case, the practical formula for linewidth reduction factor F^2 Equation 2.14 has to be considered. The comparison for the lowerest linewidth for each configuration, along with the theoretical predcition, is shown in Table 3.1.

Table 3.1.: Comparison of the linewidth reduction value achieved by laser w/ and w/o feedback, and the predicated reduction value.

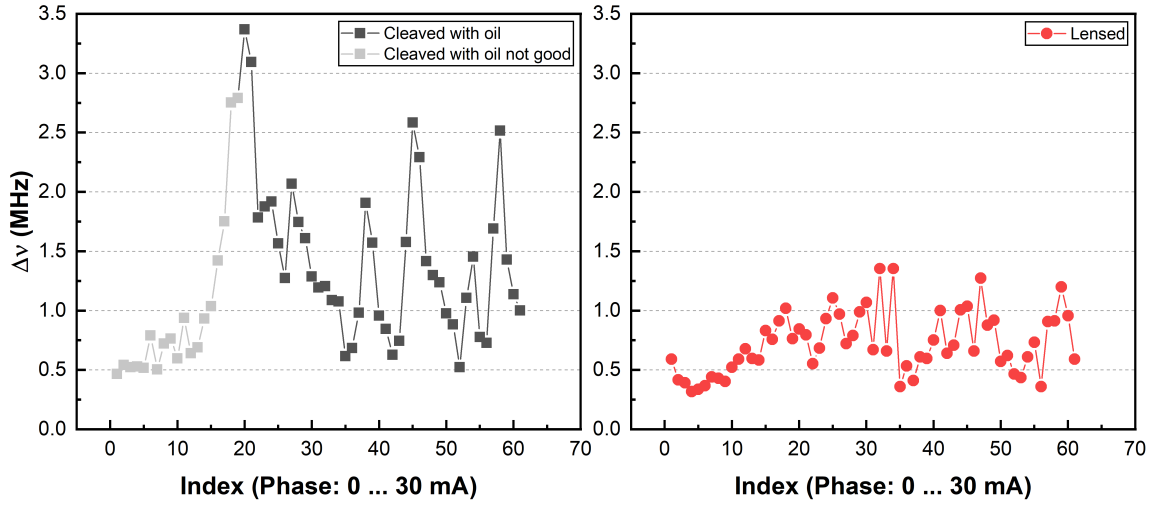|	Cleaved with oil	Lensed	Reduction	Reduction (Predicated)
$\Delta v \ (MHz)$	0.522 @ Index 52	0.317 @ Index 4	1.647	1.11

Figure 3.4.: (a) The laser linewidth without feedback from the chip facet, the light grey points indicate the bad working points, (b) laser linewidth with feedback from the chip facet, it shows a more stable behavior compare to the laser without feedback.

3.2. Relative Intensity Noise (RIN) Measurement

The measurement of relative intensity noise (RIN) describes the laser's maximum available range for signal modulation and serves as a quality indicator of laser devices. RIN is defined as the ratio of the mean-square optical intensity noise to the square of the average optical power: [cite]

$$RIN = \frac{\langle \Delta P \rangle^2}{\langle P \rangle^2} dB/Hz \tag{3.1}$$

where $\langle \Delta P \rangle^2$ is the mean-square optical intensity fluctuations (in a 1-Hz bandwidth) at a specified frequency, and $\langle P \rangle$ is the mean optical power.

In order to measure the RIN, the optical power is converted to a current after the receiving photodiode and the ratio of optical powers squared is equivalent to the ratio of the detected electrical powers. Thus, *RIN* can be expressed in terms of detected electrical powers. Equation 3.1 can be rewritten as:

$$RIN = \frac{N_{elec}}{P_{avg}(elec)} dB/Hz \tag{3.2}$$

where N_{elec} is the power-spectral density of the photocurrent at a specified frequency, and $P_{avg}(elec)$ is the average power of the photocurrent.

The noise at the receiver output results from three fundamental contributions: laser intensity noise primarily due to spontaneous light emissions; thermal noise from the electronics; and photonic shot noise. Since the photonic shot noise and the receiver thermal noise are not included in the definition of N_{elec}, they have to be subtracted from the measured *RIN* results:

$$N_{laser} = N_{elec} - N_{shot} - N_{thermal} \, W/Hz \tag{3.3}$$

By using Equation 3.2 and Equation 3.3, the value of RIN_{laser} can be determined:

$$RIN_{laser} = RIN(measured) - \frac{2e}{I_{avg}} - \frac{N_{thermal}}{P_{avg}(elec)} \tag{3.4}$$

where e is the elementary charge, I_{avg} denotes the detected average photocurrent, $N_{thermal}$ is the measured noise floor of the lightwave signal analyzer in a 1-Hz bandwidth.

The RIN comparison for the two configurations are shown in Figure 3.5. The RIN value for laser w/o feedback ranges from -144 dB/Hz to -142 dB/Hz while for lase w/ feedback it has two parts: without the spikes it ranges from -146 dB/Hz to -144 dB/Hz, which is lower than the case w/o feedback; the spikes appear in Figure 3.5 (b) are correspoinding to the additional mode hopping behavior in Figure 3.1 (b), which indicates the appearing of the undamped RO, will increase the RIN value.
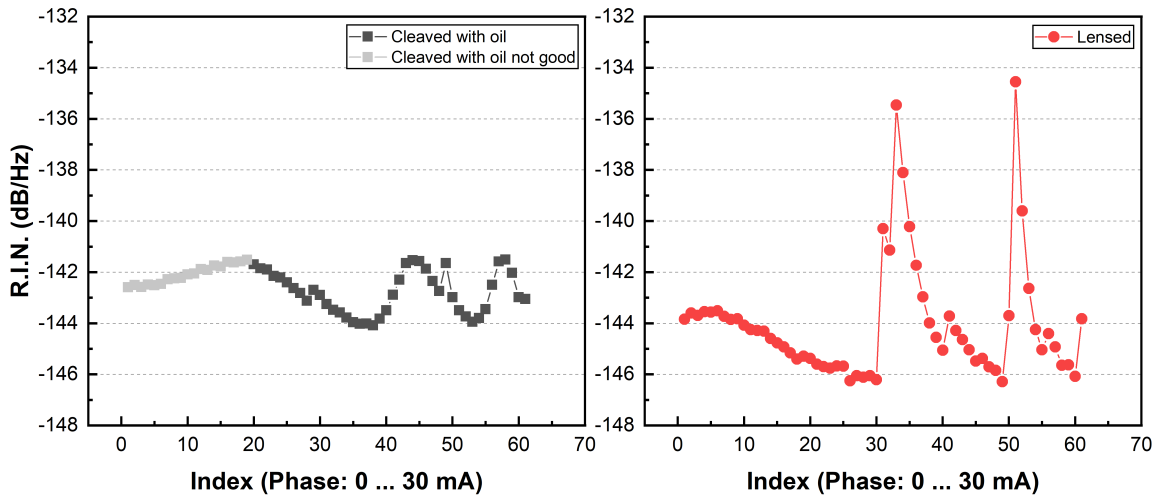

Figure 3.5.: Comparison of the RIN value for laser w/ and wo/ feedback. (a) Laser with feedback, (b) laser without feedback, the spikes indicate the appearing of the undamped RO, which increase the RIN significantly.

3.3. Bandwidth Measurement

3.3.1. Small Signal Modulation

From a practical viewpoint the quantity of interest is the modulation bandwidth ν_B which indicates the frequency range over which the laser responds to the current modulation. It is usually defined as the frequency at which the modulation response has dropped by 3 dB relative to its low-frequency or DC value [10].

The frequency response of the laser transmitter under small signal modulation is found by the usual assumption of a harmonic current modulation superimposed on a constant bias above threshold.

$$H(\omega) = \frac{\omega_R^2}{\omega_R^2 - \omega^2 - 2j\omega\gamma} \tag{3.5}$$
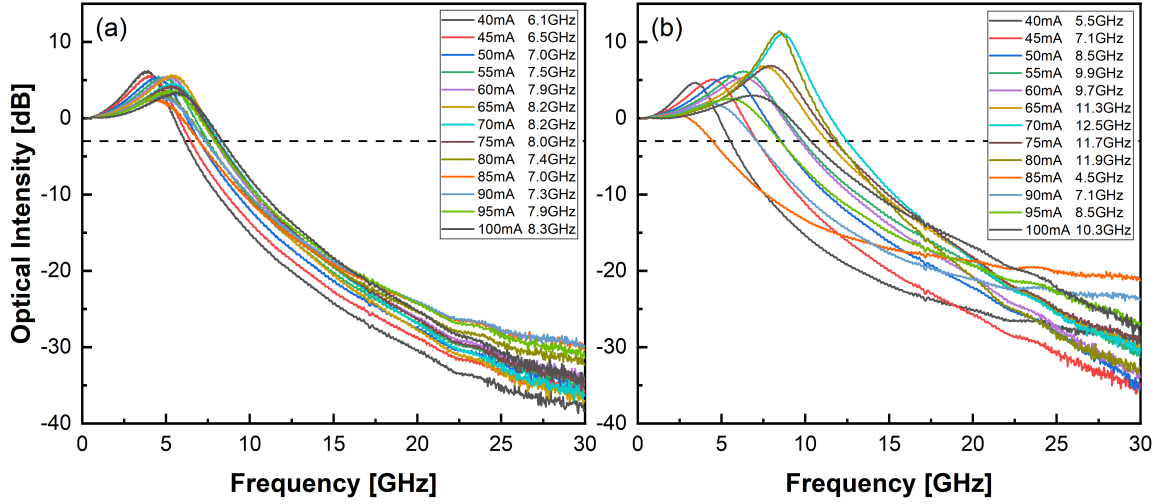
Figure 3.6.: Bandwidth measurements of a normal tunable laser. (a): Without feedback, the f_{3dB} show a normal behavior that first increase with the applied gain current and then decrease, (b): with feedback, the prominant peaks at 70 mA and 75 mA are due to the undamped RO peaks, at this condition, the f_{3dB} got increased compare with the lase without feedback.

in Equation 3.5, ω_R is the relaxation resonance frequency and γ is the damping factor.

The relaxation oscillation frequency is a measure of the maximum modulation ability in semiconductor lasers through the injection current. Above the relaxation oscillation, the modulation efficiency is greatly degraded and intensity modulation through the injection current becomes difficult. [Semiconductor Lasers. Stability, Instability and Chaos.pdf]

The laser seeks a steady-state operation which maximizes feedback. When external feedback is present, the state corresponding to maximum feedback occurs when there is phase alignment between the semiconductor cavity field and the reflected field. A carrier number change n will change the resonance frequency of the semiconductor cavity. This in turn causes a phase change ϕ between the laser field and the reflected field. This acts to decrease the light intensity in proportion to $1 - cos\phi \approx \frac{\phi^2}{2}$, which decreases the rate of stimulated emission and further increases n. This increase in n again raises the cavity resonance frequency, causing the phase misalignment ϕ to continue to grow. Instability occurs for finite fluctuations of ϕ and n when this effect becomes greater than the restoring forces giving rise to the relaxation oscillations described above.

steady-state operation (phase alignment of the cavity field and reflected field)

In steady-state operation, the laser with reflective feedback can be thought of as phase locked to the reflected field. The phenomenon that we describe is driven by large fluctuations in spontaneous emission that dislodge the laser from this locked state that is stable for small fluctuations. [Henry, Kazarinov 1986]

3.3.2. Detuend loading condition

Operating the DBR laser under the detuned loading condition was measured and the result is shown in Figure 3.7. The measurement was performed by stabilizing the device at 25 °C and using a gain current I_{gain} of 75 mA. When the laser is lasing on the slope of the grating response, the side modes have a different gain spectrum relative to the peak of the grating response, which introduces the asymmetric behavior of the side modes. In this case, when the left side mode is higher than the right one, means the lasing mode is operating at the longer wavelength side of the grating response, and vice versa. By increasing the phase current I_{phase} from 14 mA to 20 mA, the lasing mode is tuned from the longer wavelength side of the grating response to the shorter wavelength side. The maximum f_{3dB} achieved at the longer wavelength side (red curve in Figure 3.7) is 10.6 GHz and the minimum (grey curve in Figure 3.7) is 8.5 GHz.
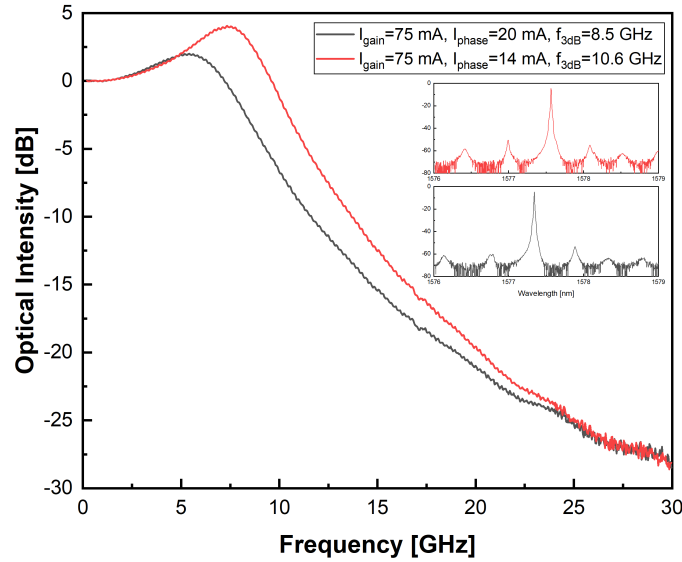

Figure 3.7.: Bandwidth enhancement with the detuned loading condition on DBR tunable laser. The red curve is detuned to the longer wavelength side of the grating response, shows an increased bandwidth of 2.1 GHz compared to the grey curve without bandwidth enhancement effect.

3.3.3. Undamped RO

For the laser under undamped RO conditions, not all the undamped behavior lead to the good performance of the laser. As shown in Figure 3.8, the appearing of the undamped RO peak leads to the carrier-photon resonance appears at a higher relaxation oscillation frequency which permits a higher f_{3dB} value. As the side peaks slowly move towards the main peak with increasing intensity, the carrier-photon resonance become stronger with a slightly decreased relaxation oscillating frequency. When more side peaks appear in Figure 3.8 (c.1), the undamped RO behavior is very strong which lead to a broder lineshape and the intensity modulation shows prominent peaks with frequency correspoinding to

the mode spacing of the side peaks. This last behavior leads to broadened lineshape and significantly decreases the f_{3dB} compare to the other two cases.
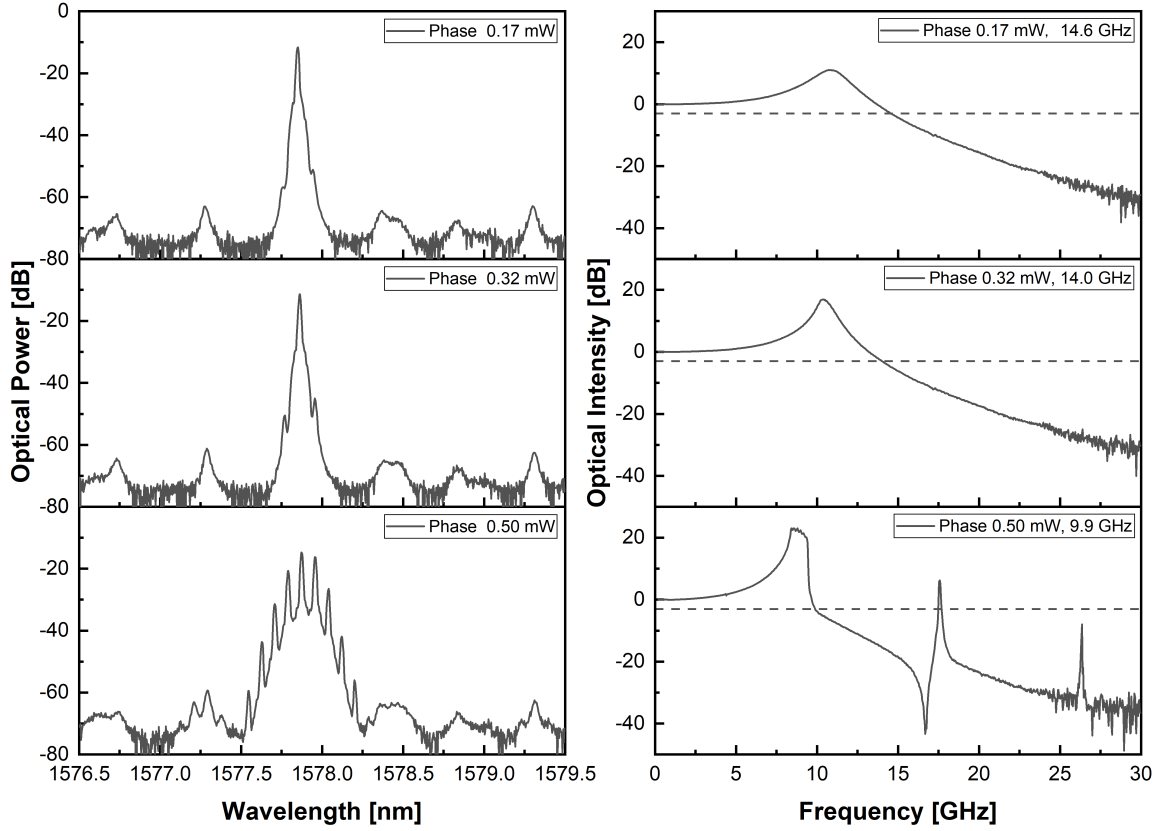

Figure 3.8.: Laser spectra and their correspoinding intensity modulation curve. (a.1) Appearing of the undamped RO peak leads to a higher carrier-photon resonance in (a.2), (b.1) growing of the side peaks leads to increase of the carrier-photon resonance peak in (b.2), (c.1) drastic undamped RO leads to broadened lineshape and decreased modualiton bandwidth in (c.2).

3.3.4.

Chirp arises because the frequency of the laser mode depends on the carrier number in the active region. Above threshold, the carrier number changes because of two effects: spectral hole burning prohibits the perfect pinning of the carrier number and permits adiabatic chirp, and during transients, there are relaxation oscillations of carrier number, which cause dynamic chirp. [Kazarinov 1987]

Current modulation of the active region results in a modulation of both the photon density and the carrier density. The modulation of the carrier density modulates the gain; however, it also modulates the index of the active region na . As a result, the optical length of the cavity is modulated by the current, causing the resonant mode to shift back and forth in frequency. [Larry A. Coldren.pdf]

If we consider the case discussed earlier where the semiconductor cavity is extended by a passive section of length L_1, with a nonreflective transition between the two sections, the reflection at the semiconductor section constant in magnitude, but has a frequency-dependent phase shift with $d\phi_r/d\omega = 2L_1/v_g1$ where $2L/v_g1$ is the roundtrip time in the external cavity. Therefore, in this case $B = 0$, the chirp reduction factor is [Kazarinov 1987]

3.4. Chirp Parameter Measurement

(α-Factor) Light chirping is a parasitic property of intensity modulated light. It originates in light emitters that produce a phase shift as the intensity is varied [11]. Semiconductor lasers exhibit a particular nonlinearity in the interaction of the light with the active medium, which distinguishes them from all other lasers. The nonlinearity originates from the physics of the semiconductor band structure, since the photon generation typically occurs due to interband transitions. The gain spectrum of such lasers therefore does not exhibit a symmetric peak, as atomic transitions do, but has a strongly asymmetric shape. This affects the dispersive properties of the lasers as well, since those properties are connected via the Kramers-Kronig relation. As a consequence, the dispersion curve for the refractive index exhibits its zero crossing at higher frequency than the maximum of the gain spectrum. If the gain changes, e.g., by a change of the carrier density, the refractive index changes as well, which would not be the case for atomic transitions. Hence, changes in gain are in semiconductor lasers associated with changes in refractive index and vice versa. Since with a change of refractive index of the medium the optical frequency and thus the optical phase changes, one also speaks of amplitude phase coupling. A small change in the intensity (induced, e.g., by a change in the injection current, by dynamical instabilities, or even a spontaneous emission event) causes an excess perturbation of the phase of the lasing mode. In the rate equation description, the effect is taken into account via the so-called α parameter, which is also referred to as Henry parameter or linewidth enhancement factor. It is defined as

$$\alpha = -\frac{d\chi_r(n)/dn}{d\chi_i(n)/dn} \tag{3.6}$$

3.4.1. Measurement with LCA

The network analyzer of Figure 3.9 measures the small-signal frequency response of a light emitter, a dispersive medium and a light receiver. The dispersive medium is 81 km of standard, single-mode fiber (zero dispersion at 1.3 μm) from and Er-doped fiber amplifiers pumped at 1.55 μm. Resonance frequencies are observed as sharp peaks in the frequency response.

The resonance frequencies f_u of Fig.2 corresponds to the uth-zeros of xx. They follow a very simple law:

$$f_u^2 L = \frac{c}{2D\lambda^2}(1 + 2u - \frac{2}{\pi}arctan(\alpha)) \tag{3.7}$$
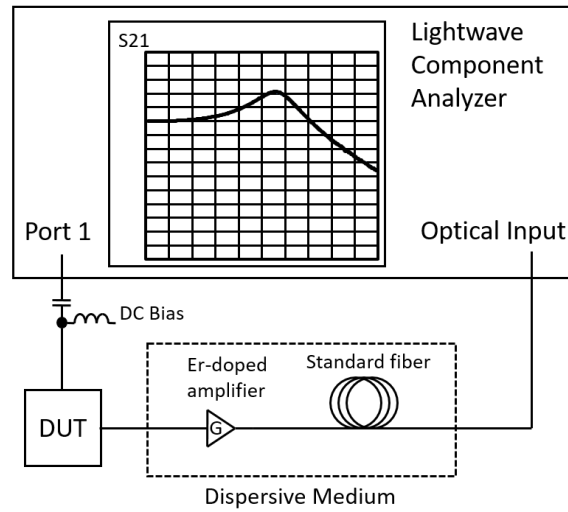
Figure 3.9.: Schematic set-up for chirp parameter measurement.

The equation is the result of two simultaneous interferences between the carrier and the two sidebands. Plotting $f_u^2 L$ versus $2u$ gives a straight line whose slope and position yield the dispersion and the chirp parameter by liner regression.

Table 3.2.: My caption

Current [mA]	α	
	w/o feedback	w/ feedback
40	3.918	2.726
50	3.821	2.328
60	3.462	2.596
70	3.897	2.984
80	3.86	4.45
90	4.078	2.997
100	3.515	2.878

3.4.2. AM-FM Index Method

The experimental arrangement for measuring the intensity and phase modulation index is shown in Fig. 1. The semiconductor laser is biased above threshold and a small sinusoidally varying current at frequency Ω is superimposed. The intensity and spectral density of the radiation field are given by

$$Intensity : E_0^2[1 + m\cos(\Omega t)] \tag{3.8}$$

$$Spectrum : Center\ line\ at\ \omega_1 : E_0^2[J_0^2(\beta) + m^2 J_1^2(\beta)] \tag{3.9}$$

$$First\ sidebands\ at\ \ \omega_1 \pm \Omega : E_0^2\{J_1^2(\beta) + 1[(m/2)(J_2(\beta) - J_0(\beta))]^2\} \tag{3.10}$$
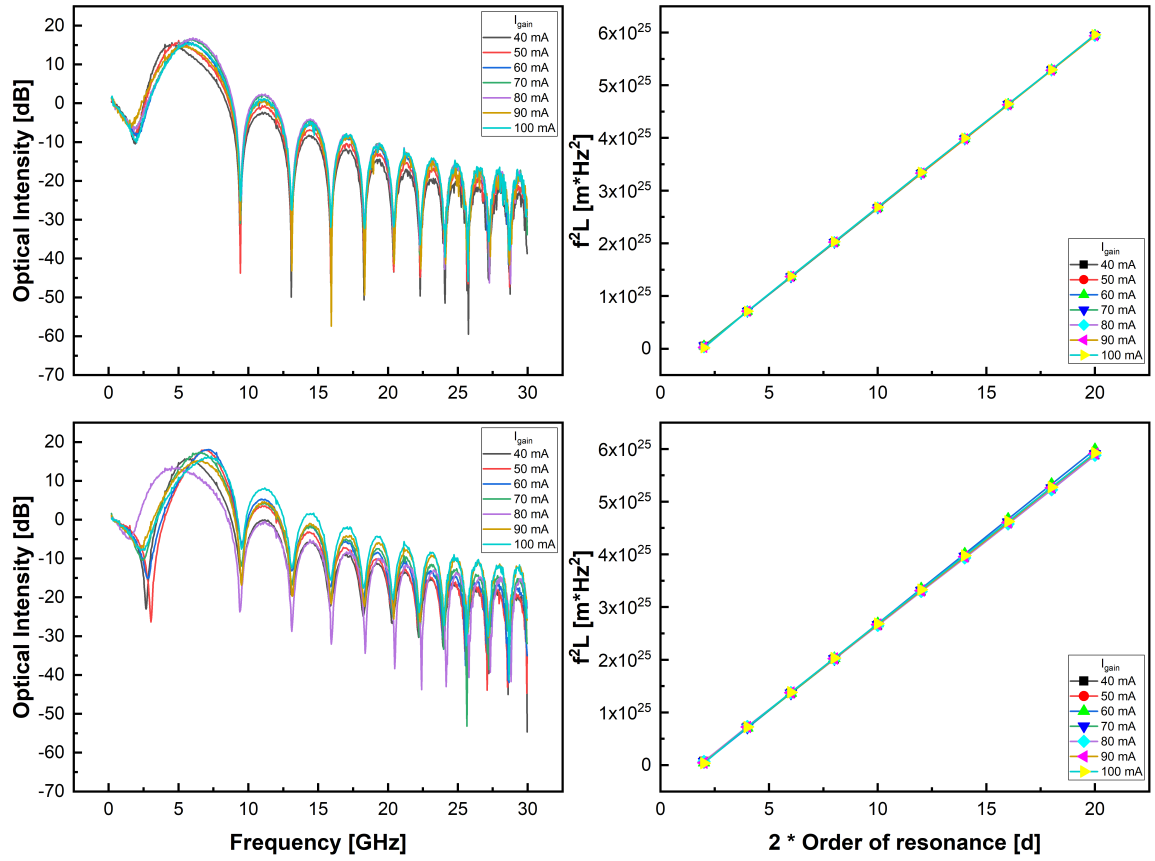
Figure 3.10.:

The phase modulation index β can be found by measuring the relative sideband strength and using Equation 3.9 and Equation 3.10. The factor α_m is then obtained as $\alpha_m = -2(\beta/m)$.
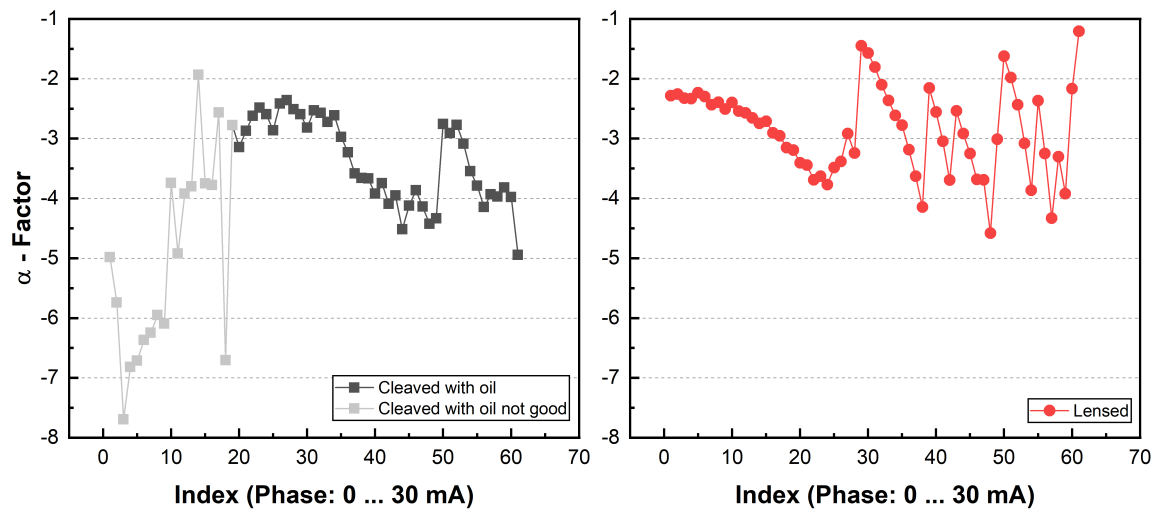
Figure 3.11.: Comparison of α parameter

3.5. Phase Noise Measurement

4. Tunable Laser with on Chip Controllable Feedback
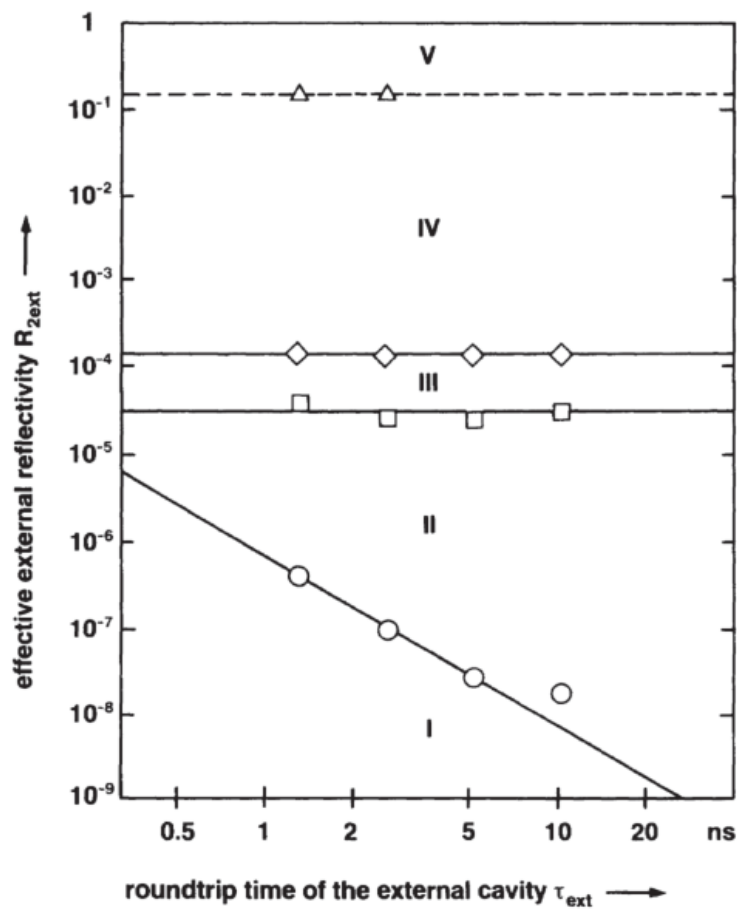
4.1. Design

Figure 4.1.: Feedback regimes for a laser diode.

4.1.1. Active and Passive Elements

As a variable optical attenuator (VOA) a 1x1 thermally tunable Multimode interferometer (MMI) is used (Fig.3.4.c). MMI is a multimode waveguide in which the light propagates

in N modes. The various modes interfere with each other and produce an interference pattern in the MMI. This pattern allows at points of constructive interference to place output waveguide and thus to tap multiple outputs, each with a corresponding proportion of the total output power from an input signal. Depending on the design of the structure, the MMI can realize a different power division. On one side along the MMI is placed an electrode that allows using the thermo-optical effect. We distinguish the states ON and OFF. In the OFF state, there is no heating of the electrodes and constructive interference takes place at the point where the output waveguide is. In ON-state, the interference pattern of the MMI is so affected, so that shifts through the partial change of the refractive index of the MMI, the position of constructive interference. Thus, a maximum interference point moves away from the position of the output waveguide and the output signal is tapped at reduced power (Fig.3.4.a and b). In this way a variable optical attenuation is created. An input waveguide with a width and height of 3.2 μm leads light into the interferometer. The height of the MMI (x-axis) also corresponds to 3.2 μm, the width is 18 μm and the length is 380 μm. The light that is leaving the MMI is received by an output waveguide. Height and width of the output waveguide coincide with the dimensions of the input waveguide. The transition of the input and output waveguide of the MMI is realized with taper sections that reduce the coupling losses. This VOA design was showing the best results compare to the literature [16-18].

4.1.2. Long Feedback Cavity

4.1.3. Short Feedback Cavity

4.2. Characterization

Table 4.1.: My caption

Current [mA]	α				
	$I_{phase} = 10\ mA$	$I_{phase} = 11\ mA$	$I_{phase} = 12\ mA$	$I_{phase} = 13\ mA$	$I_{phase} = 14\ mA$
75	1.725	2.063	2.22	2.624	3.247
75	1.818	1.991	2.296	2.618	3.257
75	1.818	2.07	2.246	2.614	3.253
75	1.808	2.054	2.242	2.566	3.221
Average	1.79225	2.0445	2.251	2.6055	3.2445

5. Conclusions & Outlook

5.1. Conclusions

5.2. Outlook

Bibliography

[1]   R Tkach and AR Chraplyvy. "Regimes of feedback effects in 1.5-μm distributed feedback lasers". In: *Journal of Lightwave technology* 4.11 (1986), pp. 1655–1661.

[2]   Larry A Coldren, Scott W Corzine, and Milan L Mashanovitch. *Diode lasers and photonic integrated circuits*. Vol. 218. John Wiley & Sons, 2012.

[3]   R Kazarinov and C Henry. "The relation of line narrowing and chirp reduction resulting from the coupling of a semiconductor laser to passive resonator". In: *IEEE Journal of quantum electronics* 23.9 (1987), pp. 1401–1409.

[4]   Kerry Vahala and Amnon Yariv. "Detuned loading in coupled cavity semiconductor lasers—effect on quantum noise and dynamics". In: *Applied Physics Letters* 45.5 (1984), pp. 501–503.

[5]   Olle Kjebon et al. "Experimental evaluation of detuned loading effects on distortion in edge emitting DBR lasers". In: *IEEE International Topical Meeting on Microwave Photonics pp.* 2002, pp. 125–128.

[6]   Junji Ohtsubo. *Semiconductor lasers: stability, instability and chaos*. Vol. 111. Springer, 2012.

[7]   U Bandelow, HJ Wunsche, and H Wenzel. "Theory of selfpulsations in two-section DFB lasers". In: *IEEE photonics technology letters* 5.10 (1993), pp. 1176–1179.

[8]   Klaus Petermann. *Laser diode modulation and noise*. Vol. 3. Springer Science & Business Media, 2012.

[9]   Ivo Montrosset and Paolo Bardella. "Laser dynamics providing enhanced-modulation bandwidth". In: *Semiconductor Lasers and Laser Dynamics VI*. Vol. 9134. International Society for Optics and Photonics. 2014, 91340H.

[10]   Govind P Agrawal and Niloy K Dutta. *Semiconductor lasers*. Springer Science & Business Media, 2013.

[11]   F Devaux, Y Sorel, and JF Kerdiles. "Simple measurement of fiber dispersion and of chirp parameter of intensity modulated light emitter". In: *Journal of Lightwave Technology* 11.12 (1993), pp. 1937–1940.

A. Appendix

A.1. Photon-photon resonance calcuation